A Diagnostic Comparison of the 1980 and 1988 U.S. Summer Heat Wave–Droughts

BRADFIELD LYON

Department of Earth Sciences, University of Massachusetts at Lowell, Lowell, Massachusetts

RANDALL M. DOLE

NOAA/ERL/CDC, Boulder, Colorado

(Manuscript received 7 March 1994, in final form 11 November 1994)

ABSTRACT

Observational analyses are performed to examine the roles of remote and local forcing in the evolutions of the extreme U.S. summer heat wave–drought cases of 1980 and 1988. At early stages, both events are associated with anomalous stationary wave patterns. Wave activity flux analyses suggest that in the 1980 case anomalous wave activity propagates southeastward from an apparent source region to the south of the Aleutians. The flux pattern is more complex in the 1988 case but suggests two possible source regions, one over the central North Pacific to the north of the Hawaiian Islands and a second located over the far western Pacific. The 1988 analyses show no anomalous wave propagation out of the eastern tropical Pacific, although this result does not necessarily preclude a role for tropical forcing in generating the anomalous wave train.

In both cases the anomalous wave trains and associated wave activity fluxes become very weak by early July, indicating that remotely forced anomalous stationary waves are unlikely to account for the later stages of the heat wave–droughts. This leads us to examine whether these events were enhanced or prolonged by changes in the local surface energy budget associated with reductions in evapotranspiration (ET) over the drought regions. Water vapor budgets show a systematic decrease in monthly mean ET from June to August during both events. Comparisons with nondrought summers support the idea that by late summer ET rates in both events are anomalously low. Estimated reductions in surface latent heat fluxes relative to the control years are approximately 50 W m^{-2} in 1980 and 20 W m^{-2} in 1988, with implied increases in sensible heating of similar magnitudes.

Overall, the results indicate the importance of both dynamical forcing from remote sources and anomalous local boundary conditions in accounting for the two extreme heat wave–drought events. The relative importance of these factors varies significantly during the evolution of the events, with remote forcing playing a predominant role at early stages and anomalous local boundary conditions assuming increasing importance at later stages.

1. Introduction

In this study, we focus on the observed characteristics and potential mechanisms contributing to two exceptionally intense U.S. heat wave–droughts that occurred during the summers of 1980 and 1988. These events had dire socioeconomic consequences for large regions of the country, and their unusual severity makes them particularly interesting cases for diagnostic study.

Chang and Wallace (1987) have emphasized the distinction between heat waves and droughts, noting that the typical timescale associated with heat waves is on the order of a week, while droughts may persist for months or even years. Although heat waves may develop in the absence of droughts, the two conditions often occur simultaneously. This is indeed the case for the two events in this study.

The tendency for drought conditions to be accompanied by above-normal temperatures is reflected in statistical studies showing negative correlations between contemporaneous monthly and seasonal mean temperatures and precipitation in summer over the midwestern United States (e.g., Madden and Williams 1978; Huang and Van Den Dool 1993). However, similar lag relations have also been observed, whereby dry springs tend to be followed by hot summers (Namias 1960; Chang and Wallace 1987), and positive feedbacks from anomalous surface boundary conditions have long been suggested as being important to the development and/or maintenance of droughts and attendant heat waves (Namias 1962, 1978, 1982, 1991).

Locally, the physical basis for such feedbacks involves changes in the surface energy balance. During anomalously dry conditions, latent heat losses from the surface due to evapotranspiration (ET) are greatly reduced. This reduction is mainly balanced by increases in sensible heating. In addition, drought conditions are often associated locally with an anomalous upper-level anticyclone, which favors subsidence, decreased cloudiness, and greater surface heating (Chang and

Corresponding author address: Dr. Randall M. Dole, NOAA/ERL/CDC, Boulder, CO 80303.

Wallace 1987). Studies also suggest that local ET is likely to be a significant source of moisture for summertime precipitation over continents (Mintz 1984; Lettau et al. 1979); a decrease in ET therefore also contributes to a potential positive feedback between heat waves and droughts by reducing the likelihood of precipitation in an already dessicated region. Sensitivity studies with numerical models have identified many of these effects in runs with specified soil moisture anomalies (Shukla and Mintz 1982; Rind 1982; Oglesby and Erickson 1989; Atlas et al. 1993).

Not all summer heat wave–droughts in the United States are associated with antecedent dry conditions, however, and anomalous large-scale circulations have been observed to precede their onset. This has led several investigators to suggest that an anomalous large-scale flow may initiate drought conditions, which are then maintained or enhanced through anomalous local feedbacks (Namias 1962, 1978, 1982; Oglesby and Erickson 1989; Wolfson et al. 1987; Trenberth and Branstator 1992).

Previous diagnostic studies of the 1980 and 1988 heat wave–droughts have generally considered separately the roles of anomalous boundary conditions within the drought region and remote effects associated with the large-scale circulation. For example, Wolfson et al. (1987) and Hao and Bosart (1987) have emphasized the role of local anomalous boundary conditions during the 1980 event, while remote influences relating to the development of the 1988 case have been investigated by Trenberth et al. (1988), Mo et al. (1991), and Palmer and Brankovic (1989).

In this study we will consider anomalies in both the large-scale circulation and local boundary conditions during different stages of the evolution of the 1980 and 1988 heat wave–droughts. We will attempt to identify possible source regions for anomalous stationary wave activity associated with these events, and will also consider changes in the surface energy balance of the drought regions through an evaluation of changes in ET.

The remainder of this paper is organized as follows. The primary datasets are described in section 2. A brief description and synoptic overview of the two events is given in section 3. Diagnostic results are presented in the following two sections, with the emphasis in section 4 on sources of anomalous stationary wave activity and in section 5 on water vapor budgets and their implications for local boundary forcing. Section 6 provides an overall summary of our findings.

2. Data

Three primary datasets are used in this study: monthly climatological station data, gridded objective analyses, and twice daily radiosonde sounding data. Climatological station data were obtained from the Environmental Data Service and include monthly precipitation reports for approximately 1400 stations in the 1980 case and 850 stations for the 1988 case.

The gridded analyses and radiosonde data were obtained from archives maintained at the National Center for Atmospheric Research (NCAR). Gridded data are derived from global National Meteorological Center (NMC) twice-daily (0000 and 1200 UTC) final analyses of geopotential heights, temperatures, and winds on a 2.5° by 2.5° latitude–longitude grid for all standard pressure levels from 1000 to 100 mb. Stationary wave flux diagnostics presented in section 4 are derived from NMC analyses from the 14-yr period 1 June 1980 through 31 May 1993; corresponding calculations performed from NMC analyses over the period from 1965 through 1988 (not shown) yielded highly similar results. Moisture flux analyses presented in the next section were computed from NMC analyses of temperature, relative humidity, and winds for the 9-yr period from January 1985 through December 1993. Missing or obviously incorrect gridded fields (see Trenberth and Olson 1988) were replaced by linearly interpolated values.

Locations of the thirty radiosonde stations used in the water vapor budget analyses are listed in the appendix. The sounding data consist of twice daily (0000 and 1200 UTC) radiosonde observations of temperature, humidity, and winds. In constructing the moisture budgets, all available mandatory and significant level data were used, typically resulting in about 40 levels of data for each sounding.

3. Case overviews

a. The 1980 case

The 1980 heat wave–drought had its largest impact on the southern Plains and lower Mississippi Valley. This event occurred following generally near-normal precipitation and below-normal temperatures in the region during spring (Wagner 1981; Namias 1982). Initiation of the event was associated with an anomalous large-scale flow pattern that developed very rapidly near the end of May (i.e., essentially within a 5-day period, Namias 1982). The subsequent anomalous flow pattern was identifiable in seasonal (June, July, and August) averages of upper-level heights (Dickson 1980; Namias 1982) and was characterized by three anomalous ridges located, respectively, over the eastern North Pacific, the southern Plains and the North Atlantic (Fig. 1). This general pattern has been observed during previous droughts in the region, most notably during the summers of 1952 to 1954 (Namias 1982).

The largest temperature anomalies in 1980 occurred during late June and July, well after drought onset, with record temperatures in several southern Plains states. For example, Dallas, Texas, recorded maximum temperatures in excess of 100°F every day in July (Wagner 1981). The drought and heat wave persisted in the area through August, with heat wave conditions

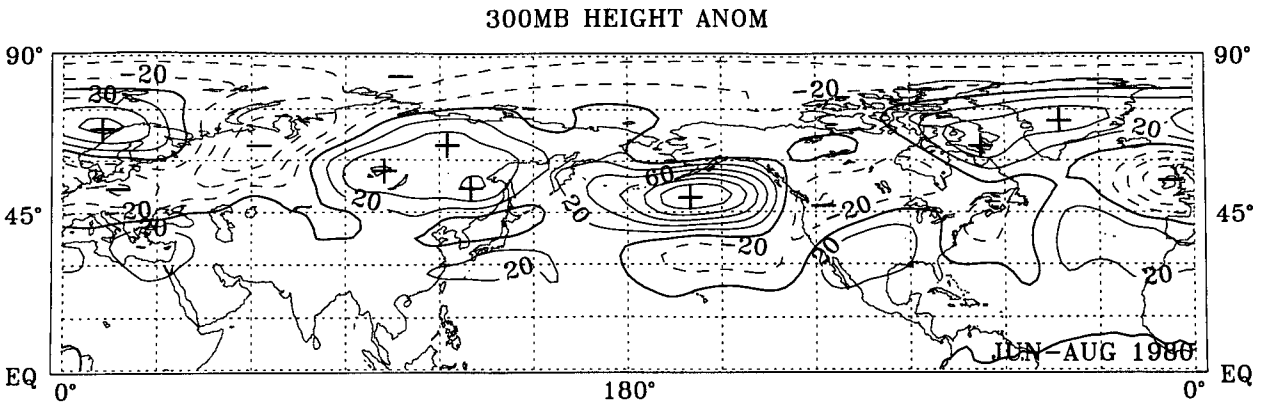

FIG. 1. Time average 300-mb height anomalies (m) for June–August 1980. Contour interval: 20 m.

in the southern Plains not breaking until the passage of a strong cold front in late September (Taubensee 1980).

Table 1 illustrates typical magnitudes of monthly mean temperature and precipitation anomalies associated with this event over the three summer months. Precipitation anomalies are expressed as a percentage of normal values over the portion of the 1980 drought region to be examined in the moisture budget analysis (cf. Fig. 12a). Temperature anomalies were computed from monthly averages for three states (Arkansas, Missouri, and Oklahoma) in the core of the drought region and were obtained by first computing individual state averages from reports of divisional temperature anomalies and then averaging over the three states. It is clear that abnormally dry and hot conditions persisted over this region throughout the summer months; indeed, examination of daily time series for individual stations (not shown) indicates that in parts of the southern Plains and southern Mississippi Valley there were only scattered light showers, with temperatures almost continuously above normal from July through mid-September. For further descriptions and details of this event, see Namias (1982), Dickson (1980), Livezey (1980), and Wagner (1980, 1981).

b. The 1988 case

The heat wave–drought of 1988 contrasted with the 1980 event in a number of respects. First, the 1988 event was preceded by an abnormally dry spring over large portions of the western and midwestern United States (Janowiak 1988; Trenberth et al. 1988). In addition, an anomalous large-scale flow pattern was observed during spring and early summer, as indicated by the 300-mb April–June time-average height anomaly pattern (Fig. 2). The large positive height anomalies centered over the northern Plains and directly associated with the heat wave–drought conditions appear to be part of a larger height anomaly pattern, which Trenberth et al. (1988) have suggested is a tropically forced wave train extending from the southeastern North Pacific to over North America. Comparison of this figure with Fig. 1 indicates that the flow patterns associated with the 1980 and 1988 heat wave–droughts are quite dissimilar in most respects, although both appear to be associated with wavetrains extending eastward from the Pacific across the United States.

The largest temperature anomalies in the 1988 case occurred during the month of June in the central and northern Plains, mainly near and to the west of the maximum positive height anomalies and at the time of maximum amplitude of the anomalous anticyclone over the United States. Abnormally hot conditions, however, continued over much of the upper Midwest throughout the summer. As one example of the continuing heat, monthly mean high temperature records were set for 69 cities in June, 37 cities in July, and 31 cities in August (Heim 1988).

The largest areal coverage of negative precipitation anomalies also occurred in June over a large region extending from the upper Midwest to the East Coast (Ropelewski 1988), mainly near and to the east of the anomalous ridge axis. During July, near to above-normal rainfall returned to most of the eastern United States, but rainfall continued to be well below normal across a large portion of the northern Plains and northern Midwest (Ropelewski 1988). By August, near to above normal rainfall also occurred over much of the upper Midwest, with scattered areas of below normal precipitation over the central and southern Plains and Mississippi River Valley. More detailed examination of precipitation time series at stations in the Midwest

TABLE 1. 1980 temperature and precipitation anomalies.

	Temperature anomalies (°C)	Precipitation (percent of normal)
June	1.0	64
July	3.2	45
August	2.6	70

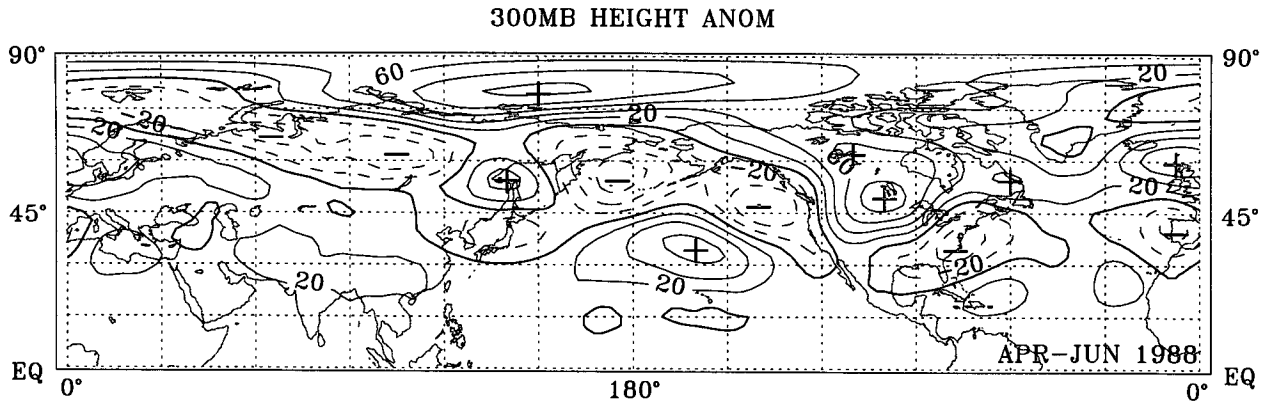

FIG. 2. Time average 300-mb height anomalies (m) for April–June 1988. Contour interval: 20 m.

shows considerable small-scale variations in August precipitation totals, with some stations receiving heavy rainfall in association with a small number of intense events, while others remained very dry [e.g., Kunkel (1989) shows August rainfall at Urbana, Illinois, at 33 mm compared to a climatological mean value of 93 mm]. These precipitation characteristics indicate the predominantly convective nature of precipitation in this period.

Table 2 illustrates typical monthly mean magnitudes of temperature and precipitation anomalies associated with this event for the three summer months. As in Table 1, precipitation anomalies are expressed as a percentage of normal values over the portion of the 1988 drought region to be examined in the moisture budget (cf. Fig. 12b), while temperature anomalies are computed from monthly averages for three states (South Dakota, Iowa, and Minnesota) near the center of the drought region. This table shows that well above normal monthly mean temperatures continued in this region throughout the summer, with abnormally dry conditions in June and July and near-normal precipitation in August.

Despite more nearly normal rainfall over the central United States by August, it would be incorrect to conclude that drought conditions had also ended over this region, as the integrated effects of the extremely dry and hot spring and early summer had by this time desiccated vegetation and severely depleted soil moisture. As one indication of this point, Palmer Hydrological Drought Indices (PDHI) showed peak areal coverage of drought conditions in July, with approximately 38% of the United States in severe to extreme drought, but by October this coverage had only been reduced to 37%, with most of the region from the northern Rockies

TABLE 2. 1988 temperature and precipitation anomalies.

	Temperature anomalies (°C)	Precipitation (percent of normal)
June	3.7	40
July	1.4	59
August	1.7	105

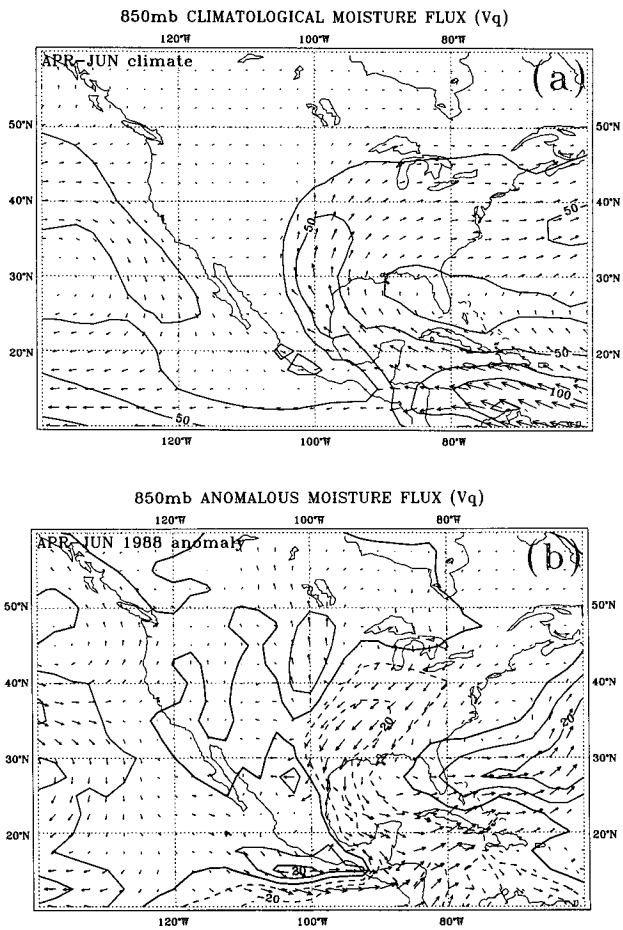

FIG. 3. (a) April–June climatological 850-mb moisture fluxes. Contour interval: 25 m s^{-1} g kg^{-1}. (b) April–June 1988 anomalous 850-mb moisture fluxes. Contour interval: 10 m s^{-1} g kg^{-1}.

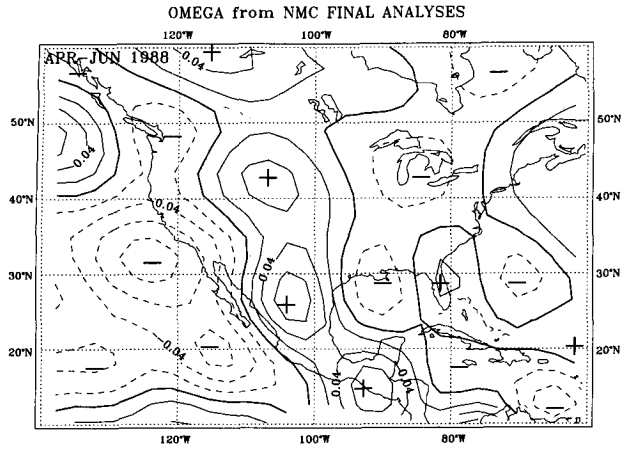

FIG. 4. Time mean vertical motion in pressure coordinates at 700 mb for April–June 1988. The values have been multiplied by −1 so that positive values correspond to ascending motion. Contour interval: 0.02 Pa s^{-1}.

eastward to the northern Mississippi Valley still experiencing severe to extreme drought conditions (Heim 1990). Large long-term precipitation deficits are evident in station data throughout the upper Midwest (not shown), with typical rainfall deficiencies for the six-month period ending 30 September in the range of 200–350 mm. Later, we will present evidence that these long-term drought conditions led to a significant reduction in evapotranspiration over the drought region by late summer and argue that this factor likely contributed significantly to the continuation of heat wave conditions in this region.

For additional descriptions of this event, see Ropelewski (1988), Trenberth et al. (1988), and Namias (1991).

c. *Relationship of flow anomalies to weather anomalies*

Before investigating potential source regions for the anomalous wave patterns associated with the two events, we will briefly discuss the relationship between the observed circulation and weather anomalies over the United States. With respect to the large-scale flow, three factors are likely to be of primary importance in producing the early stages of heat wave–drought conditions: changes in horizontal moisture transport, anomalous vertical motions, and shifts in storm tracks. In this section, we briefly discuss and illustrate the potential roles of each of these factors for the early stages of the 1988 case.

Figure 3a shows the climatological-mean April–June 850-mb moisture fluxes $\overline{\mathbf{V}q}$, where q is specific humidity and the climatological average is determined from the 9-yr period 1985–1993. Figure 3b presents the corresponding departure of the April–June 1988 moisture fluxes from the 9-yr average. Detailed moisture budgets for the drought regions will be presented in section 5; however, it is clear from these figures that the anomalous large-scale flow in 1988 opposes the northeastward moisture flux from the Gulf of Mexico, which is the primary moisture source for precipitation in much of the central and eastern United States. The anomalous fluxes evident in Fig. 3b are related to both the anomalous anticyclonic circulation centered just west of the Great Lakes and the anomalous cyclonic circulation centered off the mid-Atlantic coast.

A second major factor in producing heat wave–drought conditions over the eastern United States is enhanced subsidence occurring near and downstream of the anomalous ridge axis. This feature can be seen quite readily in Fig. 4, which shows 700-mb time-mean vertical motion in pressure coordinates, $\bar{\omega}$, for April–June 1988 obtained by the baroclinic χ-method of Sardeshmukh (1993) and kindly provided to us by B. Liebmann and P. Sardeshmukh. Large-scale descent is evident over much of the eastern half of the United States, broadly resembling the observed pattern of precipitation anomalies over this same period (Janowiak 1988; Ropelewski 1988; Heim 1990). Subsidence and associated ageostrophic circulations inhibit both large-scale and convective precipitation by several mechanisms, including midtropospheric warming and static stabilization (capping) and suppression of moisture convergence and frontogenesis by low-level divergence. Because specific humidity q generally decreases very rapidly with height, anomalous low-level divergence strongly influences vertically integrated water vapor budgets through changes in moisture-weighted divergence $q\nabla \cdot \mathbf{V}$, as will be discussed in section 5. Subsidence also favors anomalously warm surface temperatures through midlevel warming and resulting suppression of cloudiness and convection. The location at early stages of the 1988 event of the maximum warm anomalies near and upstream of the anomalous ridge axis, however, strongly suggests that anomalous warm advection plays a key role in producing heat wave conditions during this period.

A third factor that may contribute to the initiation of drought conditions is reduction in precipitation associated with synoptic-scale systems due to shifts in storm tracks. One measure of these shifts is given by the eddy kinetic energy anomalies, K'. Figure 5 shows K' at the 300-mb level for April–June 1988, where the eddies are determined from high-pass filtered data that retains periods of less than eight days. Interestingly, the K' field provides no real indication of a large suppression of high-frequency eddy activity over the eastern United States; rather, the largest anomalies are associated with enhanced high-frequency eddy activity extending across most of the Pacific at midlatitudes and suppressed eddy activity over the western to mid-Atlantic storm track region. The absence of a clear signature of suppressed high-frequency eddy activity over the central and eastern United States is not com-

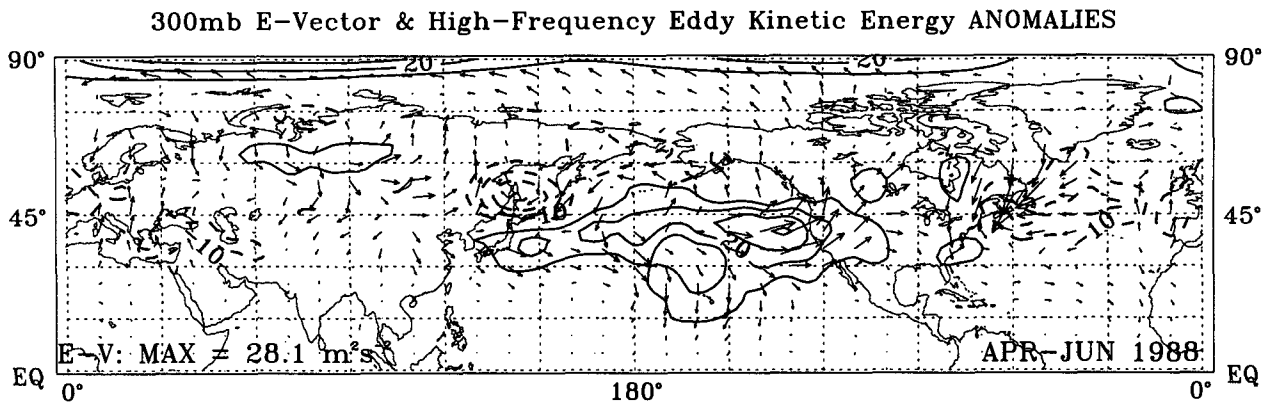

FIG. 5. April–June 1988 300-mb high-frequency eddy kinetic energy anomalies (contour interval 10 $m^2 s^{-2}$) and anomalous E-vectors.

pletely surprising, as by late May and June the climatological-mean storm track has shifted to the north of the United States border (not shown). Mesoscale and convective phenomena, which are not well captured in conventional eddy statistics, begin to play an increasingly important role in determining the distribution and intensity of precipitation over the region. These factors become increasingly evident later in the season, particularly for regions located well to the south of the mean storm tracks, as in the 1980 drought.

Figure 5 also shows corresponding anomalous *E*-vectors at the 300-mb level, where the E-vectors are obtained following Trenberth (1986), and anomalies are determined as the difference of the 1988 April–June E-vectors from the climatological mean E-vectors for the same period. The anomalous E-vector field is rather noisy but shows a large-scale pattern of divergence over the central Pacific and convergence over the central United States. This result suggests that there is an anomalous tendency for synoptic-scale eddies to force increased westerly flow in the former region, to weaken the westerlies in the latter region, and, therefore, to at least partially reinforce the existing circulation anomalies over the Pacific–North American region. The general pattern around the North American region broadly resembles E-vector patterns obtained in some blocking events, for which there is substantial evidence that anomalous eddy forcing is important in maintaining the low-frequency circulation anomalies (e.g., cf. Shutts 1986; Neilley and Dole 1991).

4. Source regions of anomalous stationary wave activity

As discussed previously, the early stages of the heat wave–droughts of 1980 and 1988 were both accompanied by anomalous stationary wave patterns. In this section, we will attempt to identify potential source regions for the anomalous stationary waves associated with these events. Our basic approach will be to apply a local conservation relation for quasigeostrophic stationary waves introduced by Plumb (1985) and applied in both model and observational studies (Plumb 1985; Mo et al. 1987; Karoly et al. 1989; Lau and Peng 1992; Black and Dole 1993; Schubert et al. 1993).

For small-amplitude waves on a zonal mean flow, the conservation relationship for stationary wave activity (Plumb 1985) may be written as

$$\frac{\partial A_s}{\partial t} + \nabla \cdot \mathbf{F}_s = C_s, \tag{1}$$

where A_s is the stationary wave activity,

$$A_s = \frac{1}{2} p \left[\frac{\bar{q}^{*2}}{\dfrac{1}{a \sin\phi} \dfrac{\partial(\bar{Q} \sin\phi)}{\partial\phi}} \right] + p \frac{E}{\bar{U}}, \tag{2}$$

$\mathbf{F}_s$ is the three-dimensional flux of stationary wave activity,

$$\mathbf{F}_s = p \cos\phi \times \begin{Bmatrix} \bar{v}^{*2} - \dfrac{1}{2\Omega a \sin 2\phi} \dfrac{\partial(\bar{v}^* \bar{\Phi}^*)}{\partial\lambda} \\ -\bar{u}^* \bar{v}^* + \dfrac{1}{2\Omega a \sin 2\phi} \dfrac{\partial(\bar{u}^* \bar{\Phi}^*)}{\partial\lambda} \\ \dfrac{2\Omega \sin\phi}{S} \left[\bar{v}^* \bar{T}^* - \dfrac{1}{2\Omega a \sin 2\phi} \dfrac{\partial(\bar{T}^* \bar{\Phi}^*)}{\partial\lambda} \right], \end{Bmatrix} \tag{3}$$

and C_s is a nonconservative source–sink term that includes diabatic and frictional effects and interactions with transient eddies. The quantities marked with asterisks represent departures from a zonal average, and the overbar represents a time-average. Here p is pressure, Q and q^* are the zonal mean and perturbation quasigeostrophic potential vorticity, U is the zonal mean flow, E is the wave energy density, u^* and v^* are the eddy zonal and meridional geostrophic wind components, a is the earth's radius, Φ is the geopotential, T is temperature, Ω is the angular rotation rate of the earth, and S is a time- and area-averaged static stability.

Plumb (1985) shows that for steady, conservative waves F_s is nondivergent and that for slowly varying, almost plane waves, F_s is parallel to the group velocity. In most applications, the starred (wave) quantities are evaluated from time averages over a reasonably long time interval, for example, a season, in which case the time-derivative term in (1) is relatively small and wave sources (sinks) are associated with regions where $\mathbf{F}_s$ is divergent (convergent). For shorter time averages, transient amplitude variations may occur in quasi-stationary (i.e., phase speed $c \approx 0$) waves, and convergence of $\mathbf{F}_s$ may also signal accumulation and growth of wave activity; Black and Dole (1993) illustrate an example of this for a case of amplifying quasi-stationary waves over the Pacific–North American region.

Figure 6a presents the 14-yr 300-mb climatological-mean Northern Hemisphere summertime (June–August) stationary waves z^* and the corresponding field of stationary wave activity fluxes $\mathbf{F}_s$. The latter are plotted only poleward of 10°N since quasigeostrophic approximations are used in their derivation. For comparison, Fig. 6b shows similar analyses for the winter season. Compared with their winter counterparts, the summertime stationary waves are considerably weaker. The wave phases also differ markedly, with the summer pattern characterized by a relative weakening of the East Asian trough and North Atlantic ridge and the development of a ridge over the interior of the United States, well east of the mean winter ridge position. As might be anticipated, the corresponding $\mathbf{F}_s$ patterns are also quite different. In comparison to their winter counterparts, summer wave activity fluxes are considerably weaker. There is little evidence of divergence of wave fluxes from the Himalayas, suggesting that, compared to winter, topographic forcing from this region is a less prominent source of stationary wave activity. Possible summertime sources of stationary waves are suggested over the eastern Pacific and Mediterranean regions, with strong southward propagation evident over both the eastern oceans in the subtropics.

Karoly et al. (1989) and Black and Dole (1993) have shown that (3) may also be applied to diagnosis potential source regions for stationary wave anomalies. In this approach, wave activity fluxes are calculated as in (3) for the zonally asymmetric part of the time-average anomaly fields. We will denote anomalous wave activity flux vectors calculated by this method by $\mathbf{F}'_s$. As discussed by Black and Dole, possible sources of anomalous stationary wave activity include diabatic heating anomalies, anomalous topographic forcing, potential vorticity advection by irrotational flow anomalies (Sardeshmukh and Hoskins, 1985), anom-

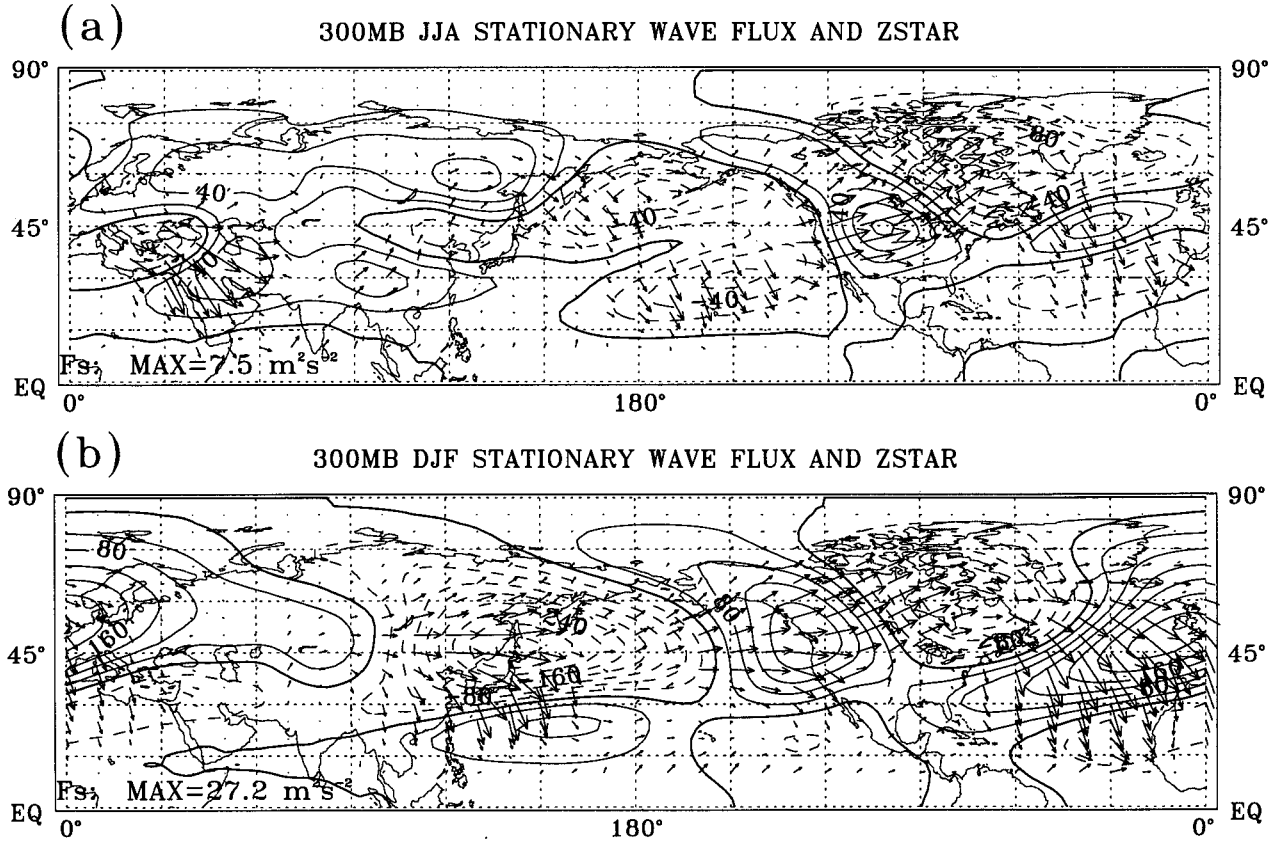

FIG. 6. Climatological 300-mb stationary waves and horizontal component of F_s for (a) summer (JJA) and (b) winter (DJF). Contour interval: 20 m for summer and 40 m for winter. Maximum $\mathbf{F}_s$ magnitude shown on bottom of plots.

alous transient eddy forcing, and interactions between the stationary wave anomalies and the climatological mean stationary waves.

Figure 7 displays the 1980 summer (June–August) 300-mb time-average height anomalies, along with $\mathbf{F}'_s$ vectors for the same period. Positive height anomalies are centered to the south of the Aleutians and over the southern Plains, with negative height anomalies located to the north of the Hawaiian Islands and over central Canada. The corresponding $\mathbf{F}'_s$ vectors diverge from near the North Pacific positive anomaly move toward the centers that appear as part of a downstream wave train, suggesting that the North Pacific near the Aleutians is a possible source region for the anomalous wave pattern.

Figure 8 displays similar monthly mean 300-mb height anomaly and $\mathbf{F}'_s$ patterns for June and July 1980. The June anomaly pattern (Fig. 8a) is quite similar to the summer mean pattern but with larger amplitude. The June $\mathbf{F}'_s$ pattern also resembles the 1980 summer mean pattern, with a strong divergence of wave activity fluxes from near the Aleutians. By July (Fig. 8b), height anomalies and associated wave activity fluxes have weakened considerably, with no evidence of anomalous wave propagation from upstream to over the heat wave–drought region. It is interesting that despite the weakening of the wave train and absence of evidence of remote forcing, some of the largest surface temperature anomalies occurred in July, and anomalously warm temperatures continued in much of the region until mid-September. These observations suggest that remote forcing alone is unlikely to account for the later stages of this heat wave–drought.

Similar analyses were performed for the 1988 event. As noted earlier, an anomalous stationary wave pattern was first observed during the spring of 1988. Figure 9 displays the April–June three-month average 300-mb height anomalies and corresponding $\mathbf{F}'_s$ pattern. As discussed earlier, the height anomaly pattern resembles a wave train emanating from the subtropical central North Pacific, with anomalous wave activity fluxes diverging from an apparent source region over the central North Pacific to the north of Hawaii. There is some indication of another anomalous wave source region near the East Asian coast, with wave activity propagating southeastward from this region into the central Pacific source region.

Trenberth et al. (1988) have suggested that the anomalous flow pattern observed in April–June 1988 is forced primarily by diabatic heating anomalies in the eastern tropical Pacific related to sea surface temperature anomalies over the same region. They support this hypothesis with results from a primitive equation, five-layer stationary wave model linearized about climatological June conditions and forced by idealized heating anomalies representing a poleward displaced eastern Pacific intertropical convergence zone (ITCZ). The specified heating anomalies consist of a zonally elongated dipole centered at 120°W, with positive (negative) heating maxima located at 15°N (5°N). Their model results suggest that the extratropical wavetrain is primarily due to the positive heating anomalies in the northern part of the dipole.

The apparent source region over the central Pacific in Fig. 9 is located well northwest of the anomalous heating region specified in the Trenberth et al. model; however, it is conceivable that due to processes such as the interaction of the forced wave with the wavy basic state, tropical heating anomalies in a linear model could give rise to a wave train with wave activity fluxes similar to those observed. In order to examine this possibility in more detail, we have calculated the wave activity fluxes associated with the stationary response to tropical heating anomalies as determined from a steady-state primitive equation model linearized about Northern Hemisphere spring and summertime mean flows.

The model results were kindly provided to us by M. Ting of the University of Illinois. A full description of the model is given in Karoly et al. (1989); however,

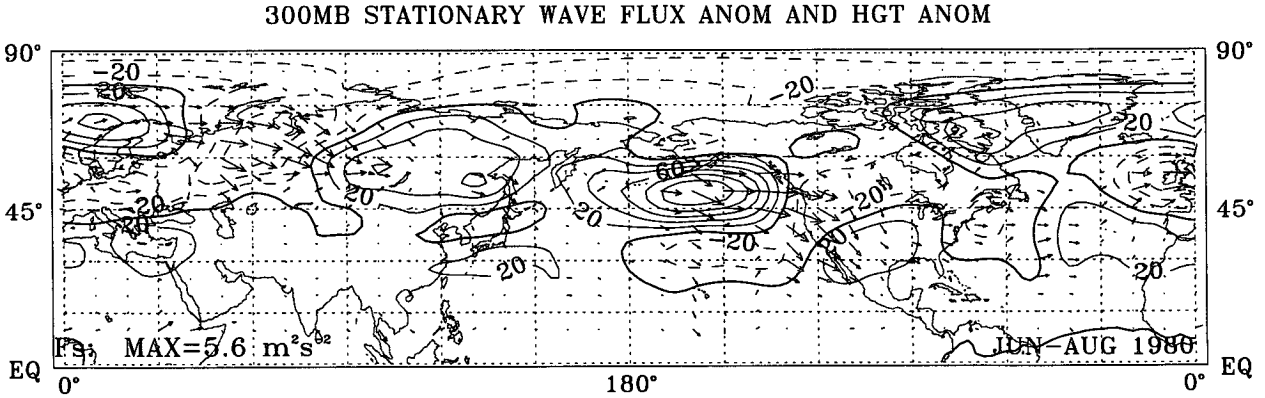

FIG. 7. Time mean 300-mb height anomalies for June–August 1980 and corresponding horizontal component of $\mathbf{F}_s$. Contour interval 20 m. Maximum $\mathbf{F}_s$ magnitude indicated on bottom of plot.

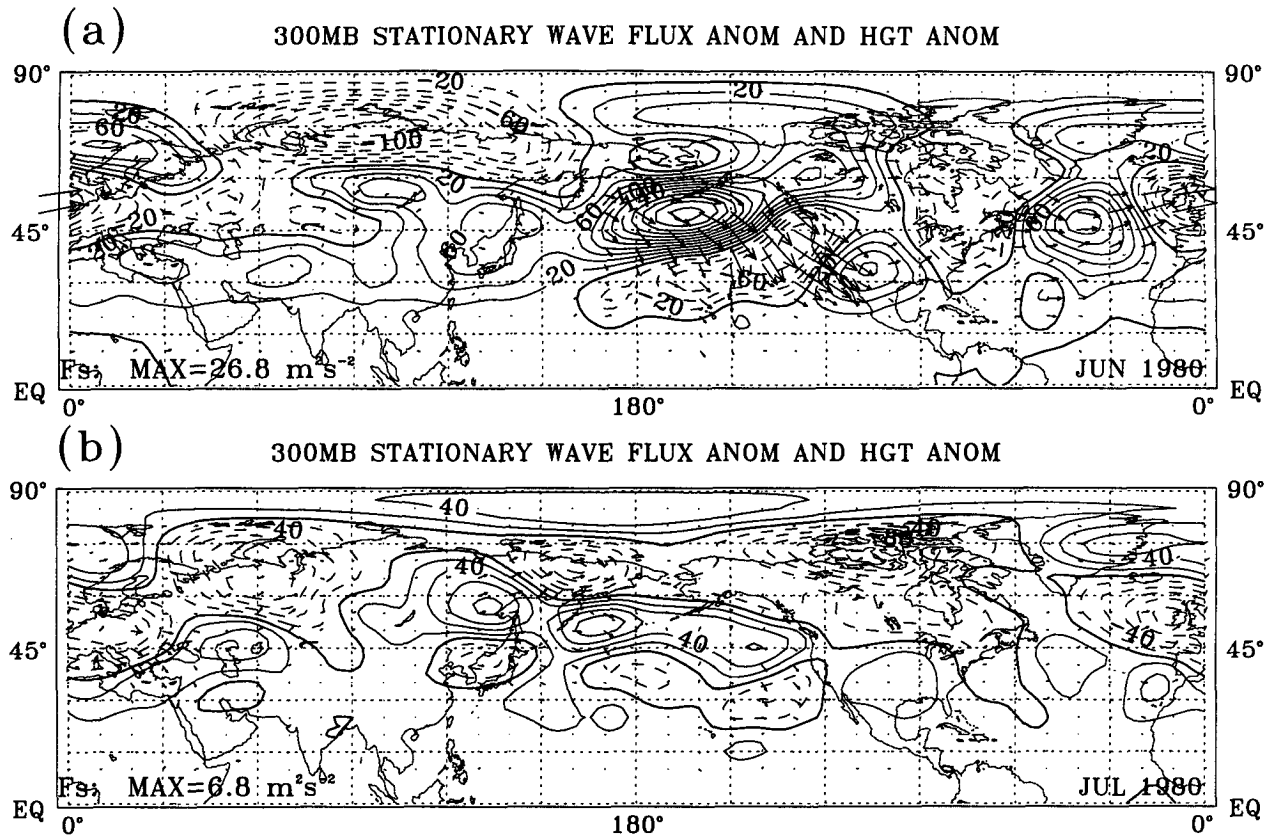

FIG. 8. As in Fig. 7 for the months of (a) June 1980 and (b) July 1980.

in brief, it is a linearized version of the GFDL spectral GCM, with nine sigma levels and a horizontal resolution of rhomboidal wavenumber 15. The thermal forcing has the same form as in Karoly et al. (1989), with a maximum vertically integrated heating of 4.5 K day^{-1}, a horizontal structure consisting of a cosine-squared bell extending to ±10° latitude and ±40° longitude from the center of the heating maximum, and a vertical structure with maximum heating at $\sigma = 0.55$ and zero heating above $\sigma = 0.1$.

Figure 10 shows the 300-mb height anomalies and corresponding anomalous wave activity fluxes F'_s for the case when the heating anomalies are centered at 10°N, 120°W, and the model is linearized about the April–June climatological time-mean flow. We have chosen 10°N rather than 15°N, as used in Trenberth et al. (1988), because the former appears nearer to the latitude of maximum eastern Pacific positive precipitation anomalies as estimated from both OLR (Trenberth et al. 1988) and MSU data (not shown). The

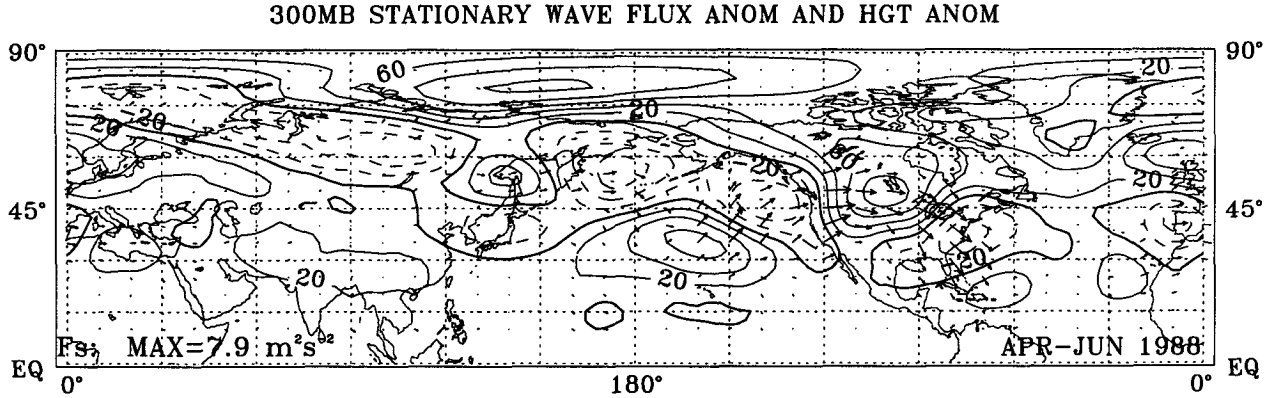

FIG. 9. As in Fig. 7 for April–June 1988.

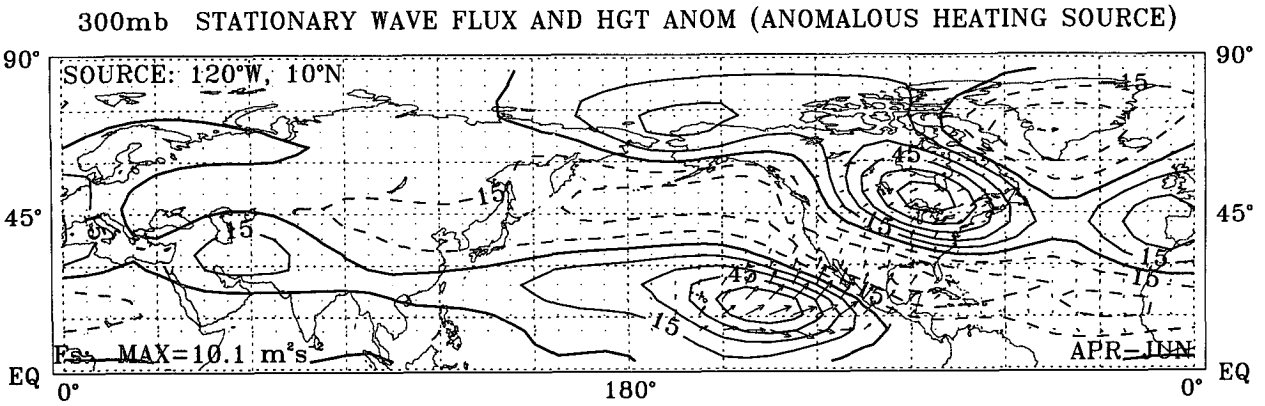

FIG. 10. As in Fig. 7 for linear model response to an anomalous heat source centered at 10°N, 120°W on a climatological April–June basic state. Contour interval: 15 m.

height anomaly pattern obtained in this model is quite similar to that shown by Trenberth et al., with positive height anomaly centers located in the eastern Pacific to the north of the heating region and to the north of the Great Lakes and negative anomalies over Greenland and over most of the north Pacific extending southeastward to the subtropical Atlantic. The anomaly pattern in Fig. 10 also closely resembles the streamfunction response patterns obtained by Lau and Peng (1992) in a barotropic model linearized about June, July, and August 250-mb climatological mean flows and forced by a dipole divergence–convergence pattern with a divergence center at 13.3°N, 120°W.

Comparisons with the observed height anomalies (Fig. 9) also show considerable qualitative similarity but differences in details. For example, the location of the Pacific anticyclone is centered well north of the Hawaiian Islands in observations, rather than east of the Islands as in the model. As a result, while observed wind anomalies over the Pacific west of 120°W and south of the negative height centers at about 15°N (Fig. 9) are predominantly westerly, model winds are easterly across the tropical Pacific, as in the Trenberth et al. and Lau and Peng model results. Differences in model and observed wave activity fluxes are more striking, with strong poleward fluxes in the model out of the tropical heating region to the east of the Hawaiian Islands that have no counterpart in the observed fluxes. In their barotropic modeling study, Lau and Peng (1992) also find anomalous poleward wave activity fluxes out of a region of divergence forcing in the eastern tropical Pacific.

Similar experiments have been performed for different base states (monthly averages from April through July) and for heating anomalies centered in a variety of different locations. A more complete description of these experiments will be given elsewhere; however, in agreement with Lau and Peng (1992), moving the heating maximum poleward also shifts the anticyclone center poleward, although the heating maxima must be shifted unrealistically far north (between 20°N and 30°N) to obtain better agreement with observations. Shifting the heating maxima northward also appears to produce stronger interactions with the wavy extratropical basic state, which Trenberth et al. and Lau and Peng note is important in amplifying their midlatitude model responses. The interactions are manifested in the wave activity fluxes by a secondary wave source near the Hawaiian Islands, although, as in Fig. 10, significant poleward fluxes continue to be evident from the primary heating region toward the United States that are not apparent in the observed fluxes.

Some caveats should be noted with regard to the observational results. First, since potential vorticity gradients along the tropopause serve as a wave guide for Rossby waves, the 300-mb level may be too low to detect a full tropical signal. However, similar calculations at the 200-mb level (not shown) yield the same qualitative F'_s pattern. Second, as the wave activity fluxes are derived from quasigeostrophic approximations, they may be less useful as a diagnostic of Rossby wave-like propagation from low latitudes, although the linear model results presented here and in Karoly et al. (1989) provide evidence that they may still provide useful diagnostic information on Rossby wave forcing and propagation. Third, as Sardeshmukh and Hoskins (1985) have noted, tropical forcing may alter the local Hadley circulation, effectively moving the stationary wave source from the Tropics to higher latitudes (Plumb 1985). The present analyses cannot exclude this possibility. The results, therefore, do not rule out a possible role of tropical forcing, although they do suggest that simple Rossby wave propagation from an anomalous heat source over the eastern tropical Pacific is unlikely to fully account for the observed 1988 April–June height anomaly pattern.

Height anomalies and $\mathbf{F}'_s$ fields were also examined for individual months during the 1988 event; Fig. 11 presents these fields for individual months from April through July. As discussed earlier, for shorter time av-

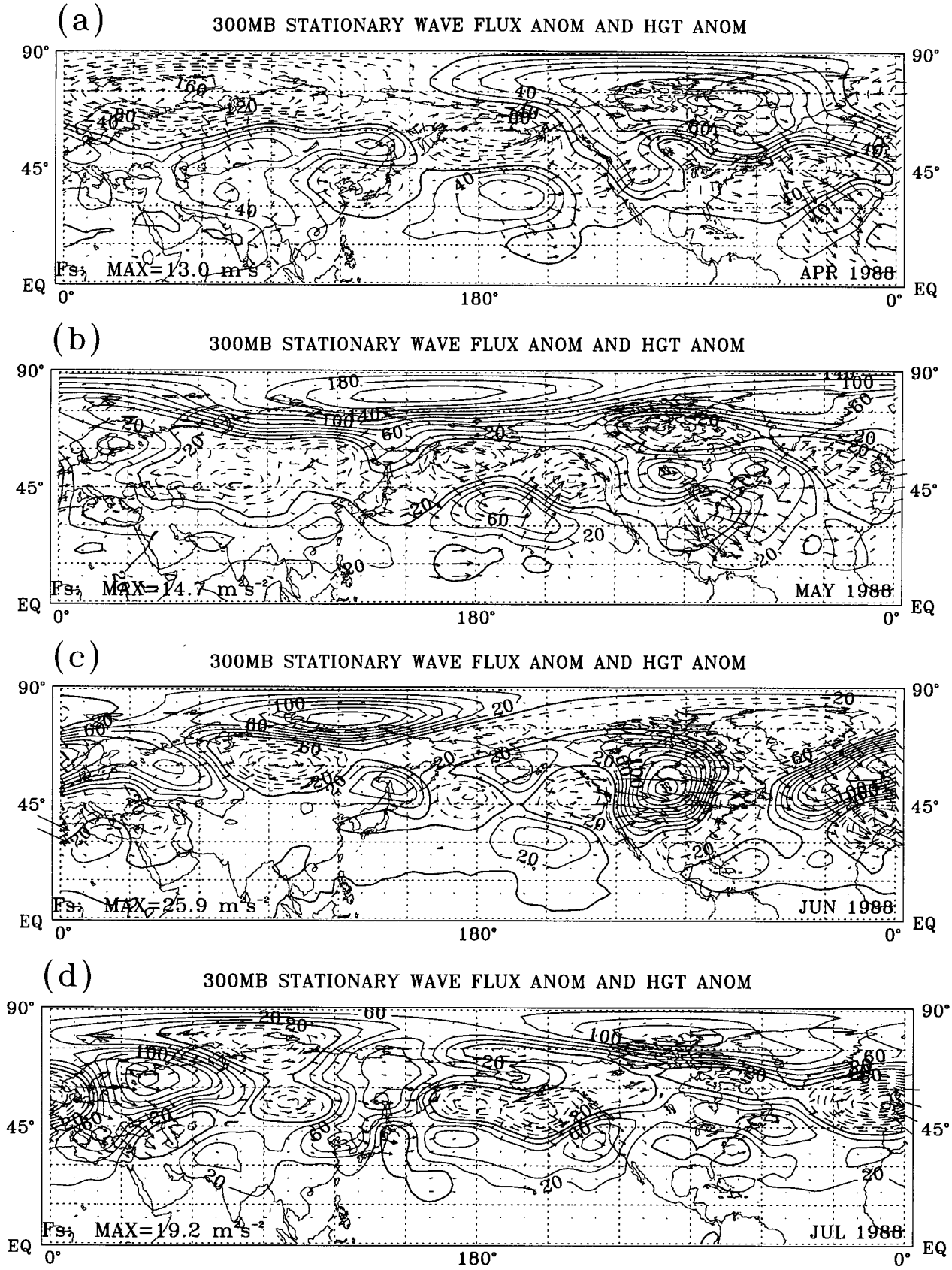

FIG. 11. As in Fig. 7 for 1988 months of (a) April, (b) May, (c) June, and (d) July. Contour interval: 20 m.

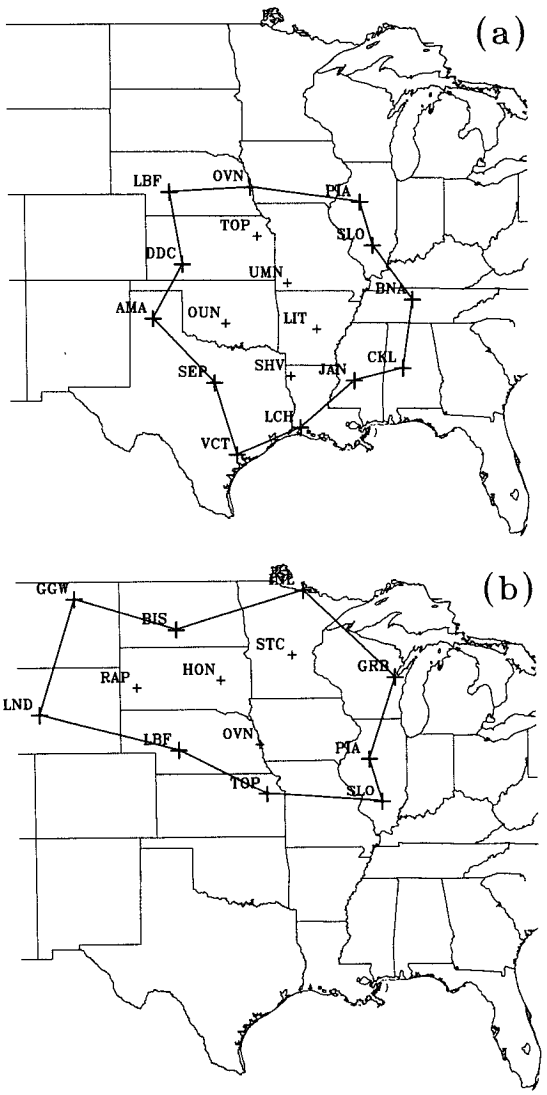

FIG. 12. Domains used in water vapor budgets for (a) 1980 event and (b) 1988 event.

erages, possible effects of transience should be considered in interpreting the $\mathbf{F}'_s$ results. Intermonthly variability is apparent in the height anomaly patterns, with the anticyclone over North America significantly more intense in June than in the other months. As in the three-month mean results, none of the monthly means shows clear evidence of anomalous wave propagation directly out of the eastern tropical Pacific, although the corresponding $\mathbf{F}'_s$ for May (Fig. 11c) suggests a possible low-latitude source to the west of the date line.

As in the 1980 case, the observed height anomaly pattern changes dramatically by July (Fig. 11d), with the wave train present at early stages of this event no longer evident. The weakening of the large positive height anomalies over the northern United States is particularly interesting since, just as in the 1980 case, the heat wave and, to a lesser extent, drought continued over this region.

5. Water vapor budgets

The previous analyses indicate that the largest flow anomalies associated with the two summer heat wave–droughts occurred during their early stages. Nevertheless, in both cases, despite a weakening of these upper-level features the heat wave and, to a lesser extent, drought persist. A possible explanation for the continued heat wave conditions is that anomalous surface boundary conditions may have acted to prolong the events. This possibility can be discussed in terms of the surface energy balance, which may be written as

$$R_N = R_L + \mathrm{SH} + \mathrm{LH} + G, \tag{4}$$

where R_N is the net incoming radiation (both shortwave and longwave), R_L is the outgoing longwave radiation from the surface, SH and LH are the sensible and latent heating, and G is a storage term indicating a gain (loss) of heat from (to) deeper soil layers. The storage term is generally much smaller than the other terms and, for present purposes, can be neglected (see Sellers 1965). Neglecting G, the net incoming solar and longwave radiation is balanced by outgoing longwave radiation and sensible and latent heat transfers. Thus, assuming R_N is approximately constant,[1] decreases in LH must be offset by increases in sensible heat transports from the surface and upward longwave radiation.

To test whether systematic decreases in latent heating occur during the evolution of the 1980 and 1988 events, we have computed water budgets over the drought regions, estimating the evapotranspiration (ET) as a residual. Twice-daily radiosonde data and monthly precipitation observations are used in this calculation. Our basic approach is similar to that of Rasmusson (1968) and Hao and Bosart (1987). We first consider the conservation of water vapor in a vertical column extending from the surface to 300 mb:

$$\frac{\partial W}{\partial t} + \nabla \cdot \mathbf{Q} = \mathrm{ET} - P, \tag{5}$$

where W is the precipitable water, Q is the horizontal water vapor flux, ET is evapotranspiration, and P is the precipitation. Taking time and areal averages of (5),

$$\langle \overline{\mathrm{ET}} \rangle = \left\langle \frac{\overline{\partial W}}{\partial t} \right\rangle + \frac{1}{A} \oint \bar{\mathbf{Q}} \cdot \mathbf{n} ds + \langle \bar{P} \rangle, \tag{6}$$

[1] The estimate of no net change in R_N is likely to be conservative due to decreased cloudiness and increased shortwave radiation received at the surface, although with reduced low-level cloudiness and moisture this is partially offset by decreased downward atmospheric longwave radiation.

where overbars represent a time average (one month), bracketed terms represent an average over the domain of area A, and $\mathbf{n}$ is a unit vector directed outward normal to the boundary of the domain. The first two terms on the right-hand side of (6) are determined from radiosonde data, while the third term is computed from archived data using roughly 1400 monthly precipitation stations for the 1980 case and 850 reports for the 1988 case. Having obtained these terms, the ET rate is calculated as a residual quantity. Figure 12 shows the domains used for both cases. The appendix gives further details of the computational methods and also provides some additional checks on the reliability of our results.

For comparative purposes, we have also obtained control values for each of the terms in (6) by performing similar analyses for months with near normal precipitation; these control values are given in Table 3. For both cases, control values were obtained as the average of seven "control months," except for July in the 1980 region, which, due to missing data in one year, is an average over six months. The control months are listed in the appendix and are characterized by near-normal precipitation values, with monthly control values between 85% and 113% of normal and seasonal mean values of 103% of normal for the 1980 case and 99% of normal for the 1988 case.

Figure 13 shows the July–August monthly mean ET rates and corresponding control values for the 1980 case, while Table 4 gives the values of the individual terms in (6) for each summer month in 1980 along with the relative rankings of these values over all years (drought + controls). Figure 13 indicates that through the summer of 1980 there a steady decline in ET rates, with the larger control values remaining nearly constant. This is similar to the result found by Hao and Bosart (1987) for a slightly different region. The estimated June to August decrease in ET represents roughly a 50 W m^{-2} decrease in latent heat fluxes from the surface over the period. This reduction in latent heat fluxes must be largely balanced by increased upward sensible and radiative fluxes, with the former

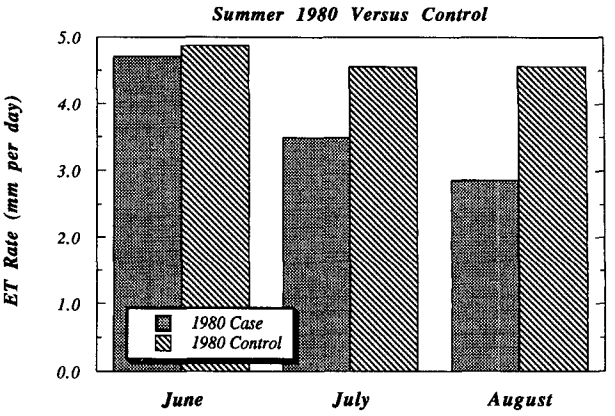

FIG. 13. Monthly mean ET rates for the 1980 case (shaded) and 1980 controls (hatched). Units are millimeters per day.

contributing to enhanced warming of the lower troposphere.

Table 4 shows that at early stages in the drought the water vapor flux divergence is the largest of any the eight (drought + control) years but becomes much reduced by late in the drought. The anomalously large water vapor flux divergence at early stages is consistent with the discussion in section 3 on the effects of anomalous moisture advection and low-level divergence on the moisture budget and supports the interpretation that large-scale processes play the key role in suppressing precipitation at early stages of the drought. The ET rate during June 1980 is not particularly anomalous, indicating that it is unlikely to be a major factor at the early stages of the heat wave–drought. At later stages, however, with continuing depletion of soil moisture and dessication of vegetation, ET decreases significantly relative to the controls; by August it is the lowest of any of the eight years. It is interesting that at later stages, although there is anomalous moisture flux convergence over the region (suppressed divergence), precipitation continues to be much below normal. Together with the anomalously low ET rates, this suggests that in this

TABLE 3. Control values of water vapor budget terms. (Units: mm day^{-1})

	1980 Region			
	Precipitable water change	Water vapor flux divergence	Precipitation	Evapotranspiration
June	0.19	0.92	3.76	4.87
July	0.13	1.28	3.14	4.55
August	−0.08	1.62	3.02	4.56
		1988 Region		
June	0.25	−0.31	3.09	3.03
July	0.10	0.04	2.65	2.84
August	−0.13	−0.41	2.73	2.18

case reductions in local evapotranspiration and associated precipitation recycling (e.g., Brubaker et al. 1993) over this region may contribute significantly to the prolongation of drought conditions.

Figure 14 and Table 5 show similar analyses for the 1988 case. Relative to control years, the June–August change in ET represents roughly a 20 W m^{-2} decrease in latent heat fluxes. This estimated reduction of ET in August is close to that obtained by Kunkel (1989) based on changes in a local surface energy budget for an Illinois corn field and to an estimate of 0.7 mm day^{-1} he obtains from a soil moisture model over a slightly different region for the period 1 July–18 August (Kunkel, personal communication, 1994). Table 5 indicates that, just as in the 1980 case, at early stages of the 1988 drought there is strongly enhanced water vapor flux divergence (again largest of the eight years) and near-normal ET rates. The anomalously large moisture flux divergence relative to the control years suggests that, as in the 1980 case, large-scale processes are playing a key role in suppressing rainfall at early stages of the drought.

In terms of the surface energy budget, the apparent decrease in ET rates found for both the 1980 and 1988 cases is significant. Henning (1989) indicates that midsummer values of the net incoming radiation in these regions is approximately 150 W m^{-2}. Thus, for both heat wave–drought cases the observed perturbations to the surface energy balance are apparently substantial, being largest during the month of August for both events. A rough estimate of the corresponding heating rates per unit mass can be obtained from

$$\frac{J}{c_p} \approx \frac{L_c \delta m_w g}{c_p \delta p}, \tag{7}$$

where J is the heating rate, δm_w is the change in water mass in an atmospheric column of a 1 m^2 cross section due to changes in ET, δp is the pressure thickness of the layer over which the heating occurs, and all other notation is standard. Assuming that the decrease in ET is mainly balanced by an increase in sensible heating that is distributed over a boundary layer of thickness δp = 150 mb, the corresponding heating rate due to reduction in ET over the drought regions is approximately 2.8 K day^{-1} for the 1980 case and 1.1 K day^{-1} for the 1988 case. Comparisons with the observed temperature anomalies (Tables 1 and 2) implies corresponding establishment times for the observed monthly temperature anomalies of ~1–2 days. These results strongly support the idea that at the later stages of the events, changes in the surface energy balance due to decreases in ET are likely to contribute significantly to the intensity and persistence of heat wave conditions despite the absence of notably anomalous stationary waves.

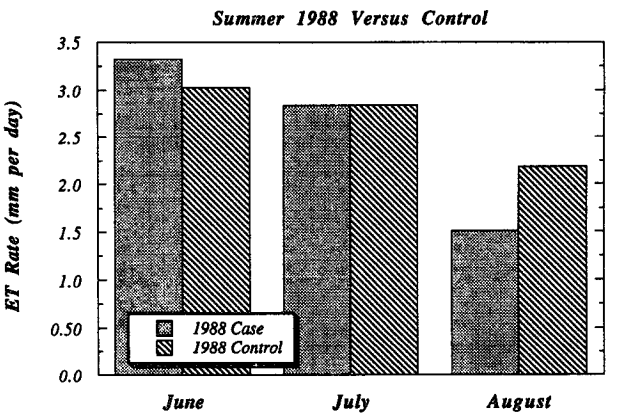

FIG. 14. As in Fig. 13 for the 1988 case and controls. Units are millimeters per day.

6. Summary and conclusions

We have investigated the roles of large-scale circulation anomalies and anomalous surface boundary conditions on the development and maintenance of two major heat wave–drought events. In their initial stages, both events were associated with anomalous stationary wave patterns that apparently emanated from upstream sources over the Pacific, although the upstream stationary wave anomalies for the two cases differed markedly. To identify potential source regions for the anomalous stationary waves, diagnostic analyses of stationary wave activity were performed following a technique developed by Plumb (1985). In the 1980 case, anomalous stationary wave activity propagated southeastward from an apparent source region to the south of the Aleutians. The wave flux pattern was more complex in the 1988 case but suggested two possible source regions, one over the central Pacific to the North of the Hawaiian Islands and a second over the far western Pacific.

To determine whether forcing from the eastern tropical Pacific might be expected to produce wave

TABLE 4. 1980 case values of water vapor budget terms and rank (from lowest to highest value). (Units: mm day^{-1})

	Precipitable water change	Water vapor flux divergence	Precipitation	Evapotranspiration
June	−0.10 (2/8)	2.53 (8/8)	2.28 (1/8)	4.71 (3/8)
July	−0.07 (4/7)	2.21 (6/7)	1.35 (2/7)	3.49 (3/7)
August	0.24 (7/8)	0.75 (2/8)	1.87 (1/8)	2.86 (1/8)

TABLE 5. 1988 case values of water vapor budget terms and rank (from lowest to highest value). (Units: mm day^{-1})

	Precipitable water change	Water vapor flux divergence	Precipitation	Evapotranspiration
June	0.21 (4/8)	1.65 (8/8)	1.46 (1/8)	3.32 (6/8)
July	0.25 (5/8)	1.03 (8/8)	1.56 (1/8)	2.84 (4/8)
August	−0.45 (2/8)	−0.59 (4/8)	2.55 (4/8)	1.51 (1/8)

activity fluxes similar to those observed in 1988, we calculated wave activity fluxes associated with the stationary response to heating anomalies in this region obtained from a steady-state primitive equation model linearized about Northern Hemisphere spring and summertime mean flows. The model results showed strong poleward fluxes out of the tropical heating region to the east of the Hawaiian Islands that had no counterpart in the observed fluxes. Although potential shortcomings of the wave flux diagnostic technique, as discussed in section 4, prevent a definitive conclusion, the present results do suggest that simple Rossby wave propagation from an anomalous heat source over the eastern tropical Pacific is unlikely to fully account for the observed 1988 April–June height anomaly pattern. This does not, however, preclude a possible role of anomalous tropical forcing in the 1988 event, either from other regions, as suggested by the May 1988 wave flux analyses, or through indirect effects, such as through excitation of an instability of the climatological basic state flow (Mo et al. 1991; Lau and Peng 1992). In addition, E-vector analyses for the 1988 case suggest a possible role of anomalous transient eddy forcing in maintaining the observed flow anomalies over the Pacific–North American region.

In both events, the anomalous wave trains and associated wave activity fluxes become very weak by early July, indicating that remotely forced anomalous stationary waves are unlikely to account for the later stages of the heat wave–droughts. We therefore examined the possibility that these events were enhanced or prolonged by changes in the local surface energy budget associated with reductions in evapotranspiration (ET) over the drought regions. At early stages of the events, ET rates were not notably anomalous compared to control years, thus providing evidence that local boundary effects were probably unimportant initially. At later stages, however, ET rates were significantly lower than controls, and estimates of anomalous heating rates suggested that anomalous boundary conditions could have been quite important in maintaining the heat wave conditions. In addition, the moisture budget results for the 1980 case indicate that reduced evapotranspiration may have also contributed to continuing drought conditions by inhibiting precipitation recycling from local moisture sources within the drought region.

On the basis of our analyses, we conclude that dynamical forcing from remote sources and anomalous local boundary conditions both contributed significantly to the heat wave–droughts, although the relative importance of these factors varied substantially during the evolution of the events. Specifically, our results suggest that remote forcing played a predominant role at early stages of the events, while anomalous local boundary forcing became increasingly important at later stages. This leads us to concur with the view frequently stated by Namias (e.g., 1989, 1991) that multiple factors, rather than a single cause, are necessary to understand the evolution of major heat wave–droughts such as occurred in 1980 and 1988. We are optimistic that through a combination of observational diagnostic analyses, simple modeling studies, and general circulation model experiments, such an understanding will continue to emerge.

Acknowledgments. Much of this work formed a part of the first author's thesis research at MIT. We gratefully acknowledge Brant Liebmann and Prashant Sardeshmukh of CIRES for providing us with their vertical motion analyses, Mingfang Ting of the University of Illinois for allowing us to use her model results, and Dennis Shea, Will Spangler, and Dennis Joseph of NCAR for their help in obtaining data used in this study. We thank the three anonymous reviewers, Ken Kunkel of the Midwestern Climate Center, Jeff Whitaker of CIRES, and Steven Feldstein of the Pennsylvania State University for their helpful comments on an earlier version of this manuscript. We also express our appreciation to Kriste Paine of CIRES for her considerable help in preparing the figures and to Marty Hoerling of CIRES for useful discussions on this work. Support for this research was provided by NASA Grant NAG5-927, National Science Foundation Grant NSF 8820938-ATM, and the NOAA Office of Global Programs.

APPENDIX

Water Vapor Budgets

a. Domains

The horizontal domains for the water vapor budget studies of the 1980 and 1988 heat wave–drought cases

consist of polygons defined by the radiosonde stations indicated in Fig. 12. These regions roughly coincide with the areas where the largest seasonal temperature anomalies were observed during the two events. The names and locations of the stations used for the two cases are listed below.

1980 Region

Station	Station name	Latitude	Longitude
72562	North Platte, NE	41°08′	100°41′
72553	Omaha, NE	41°22′	96°01′
72532	Peoria, IL	40°40′	89°41′
72433	Salem, IL	38°39′	88°58′
72327	Nashville, TN	36°07′	86°41′
72229	Centerville, AL	32°54′	87°15′
72235	Jackson, MS	32°19′	90°05′
72240	Lake Charles, LA	30°07′	93°13′
72555	Victoria, TX	28°51′	96°55′
72260	Stephenville, TX	32°13′	98°11′
72363	Amarillo, TX	35°14′	101°42′
72451	Dodge City, KS	37°46′	99°58′
72456	Topeka, KS	39°04′	95°38′
72357	Norman, OK	35°00′	97°30′
72349	Monet, MO	36°53′	93°54′
72247	Shreveport, LA	32°31′	93°45′
72340	Little Rock, AR	34°44′	92°14′
72768	Glasgow, MT	48°13′	106°37′
72764	Bismark, ND	46°46′	100°45′
72747	Internationa Falls, MN	48°34′	93°23′
72645	Green Bay, WI	44°29′	88°08′
72532	Peoria, IL	40°40′	89°41′
72433	Salem, IL	38°39′	88°58′
72456	Topeka, KS	39°04′	95°38′
72562	North Platte, NE	41°08′	100°41′
72576	Lander, WY	42°49′	108°44′
72662	Rapid City, SD	44°03′	103°04′
72654	Huron, SD	44°23′	98°13′
72553	Omaha, NE	41°22′	96°01′
72655	Saint Cloud, MN	45°33′	94°04′

b. Method of computing evapotranspiration

Monthly evapotranspiration (ET) rates are estimated from the relation shown in (6); namely,

$$\langle \overline{\mathrm{ET}} \rangle = \left\langle \frac{\overline{\partial W}}{\partial t} \right\rangle + \frac{1}{A} \oint \bar{\mathbf{Q}} \cdot \mathbf{n} ds + \langle \bar{P} \rangle, \quad \text{(A1)}$$

where overbars in (A1) indicate a monthly mean, brackets indicate an average over the domain of area A, W is the precipitable water, $\mathbf{Q}$ is the horizontal water vapor flux, $\mathbf{n}$ a unit vector directed outward normal to the boundary of the domain, E is the evapotranspiration, and P is precipitation. The precipitable water W is defined as

$$W = \frac{1}{g} \int_{p_t}^{p_s} q dp, \quad \text{(A2)}$$

where g is gravity, q is the specific humidity, p_s is the surface pressure, and p_t is the pressure at the top of the domain set at 300 mb. The horizontal water vapor flux term $\mathbf{Q}$ is defined as

$$\mathbf{Q} = (Q_\lambda, Q_\phi) \quad \text{where} \quad Q_\lambda = \frac{1}{g} \int_{p_t}^{p_s} qu dp$$

$$\text{and} \quad Q_\phi = \frac{1}{g} \int_{p_t}^{p_s} qv dp, \quad \text{(A3)}$$

where u and v are, respectively, the zonal and meridional wind components. Before computing the terms on the right-hand side of (A1), linear vertical interpolation was used to construct twice daily (0000 UTC and 1200 UTC) soundings with values of specific humidity and wind specified every 25 mb from the surface to 700 mb and every 50 mb from 700 to 300 mb for

each radiosonde observation in our domain. Significant level temperature and humidity data were employed in the construction of the interpolated soundings. Missing station data were not interpolated.

The area-averaged monthly mean precipitable water change was calculated from the average daily change (0000 to 0000 UTC) of all the stations in the domain for a given month. The water vapor flux divergence was evaluated by first computing the monthly mean value of **Q** at each radiosonde station and then computing the line integral around the periphery of the domain, using linear interpolation to obtain mean **Q** values between stations. The mean precipitation was determined from monthly precipitation data at roughly 1400 stations for the 1980 case and 850 for the 1988 case, with each station report given equal weight in the overall mean.

c. *Control ET rates*

For each month (June, July, and August) the control values of (A1) listed in Table 1 were obtained from averages for seven months obtained from years having near-normal precipitation, except for July for the 1980 region, where only six months were used due to missing radiosonde data. The years used to obtain the control values are for the 1980 region: 1978 (no July), 1979, 1981, 1982, 1985, 1986, and 1987; and for the 1988 region: 1978, 1979, 1980, 1982, 1983, 1984, and 1985. The control seasonal average values for precipitation expressed as a percentage of normal were 103% for the 1980 region and 99% for the 1988 region.

d. *Additional checks on ET rates*

Some additional checks were performed on the reliability of our ET rates. First, evaporation data were obtained for "pan" stations located within our two drought regions. A 12-yr (1977–1988) climatology of monthly mean evaporation rates for May to September was constructed at six stations, three in each of the 1980 and 1988 drought domains. These pan measurements represent a potential evapotranspiration rate since an unlimited amount of water is available to evaporate. They in fact typically overestimate the maximum surface evaporation rate for two reasons: (i) the shallow water reservoirs allow the water temperature to be artificially high, increasing evaporation, and (ii) the pan is raised above the ground surface, artificially increasing ventilation rates (Kunkel, personal communication, 1994). A typical value for the overestimate relative to a free-water surface or freely transpiring vegetated surface is about 30% (Farnsworth and Thompson 1982). Month by month comparisons of drought ET rates with the climatological pan evaporation rates (not shown) indicate our estimated drought ET rates are all considerably less than their corresponding pan values, as would be expected. Additionally, we have compared the drought ET rates with the climatological ET rates over North America presented by Henning (1989). Henning's climatological values are for the period 1930 to 1960 and were computed using the surface energy balance method of Albrecht (1965). We find our seasonal (June, July, and August) ET rates for both the 1980 and 1988 cases to be comparable in magnitude to this climatology, if not slightly lower. We note also that the period 1930–1960 used in computing Henning's climatology contains some of the most intense droughts recorded in the Great Plains, which may bias his rates toward the low side.

REFERENCES

Albrecht, F., 1965: Untersuchungen des Warme und Wasserhaushaltes der Sudlichen Kontinente. *Ber. Dtsch. Wetterdienstes,* **14**(99), 54 pp.

Atlas, R., N. Wolfson, and J. Terry, 1993: The effect of SST and soil moisture anomalies on GLA model simulations of the 1988 U.S. summer drought. *J. Climate,* **6,** 2034–2048.

Black, R. X., and R. M. Dole, 1993: The dynamics of large-scale cyclogenesis over the north Pacific Ocean. *J. Atmos. Sci.,* **50,** 421–442.

Brubaker, K. L., D. Entekhabi, and P. S. Eagleson, 1993: Estimation of continental precipitation recycling. *J. Climate,* **5,** 1077–1089.

Chang, F. C., and J. M. Wallace, 1987: Meteorological conditions during heat waves and droughts in the United States Great Plains. *Mon. Wea. Rev.,* **115,** 1253–1269.

Dickson, R. R., 1980: Weather and circulation of June 1980—inception of a heat wave and drought over the central and southern Great Plains. *Mon. Wea. Rev.,* **108,** 1469–1474.

Farnsworth, R. K., and E. S. Thompson, 1982: Mean monthly, season and annual pan evaporation for the United States. NOAA Tech. Rep. NWS34, Washington, D.C.

Hao, W., and L. F. Bosart, 1987: A moisture budget analysis of the protracted heatwave in the southern Plains during the summer of 1980. *Wea. Forecasting,* **2,** 269–288.

Heim, R. R., 1988: About that drought. *Weatherwise,* **41,** 266–271.

——, 1990: The 1988 drought in the United States: overview and historical perspective. *The 1988 United States Drought: Workshop Report.* [Available from Department of Meteorology, University of Maryland, College Park, MD 20742.]

Henning, D., 1989: *Atlas of the Surface Heat Balance of the Continents.* Gebrueder Borntraeger, 402 pp.

Huang, J., and H. M. Van den Dool, 1993: Monthly precipitation—Temperature relations and temperature prediction over the United States. *J. Climate,* **6,** 1111–1132.

Janowiak, J. E., 1988: The global climate for March–May 1988: The end of the 1986–87 Pacific warm episode and the onset of widespread drought in the United States. *J. Climate,* **1,** 1019–1040.

Karoly, D. J., R. A. Plumb, and M. Ting, 1989: Examples of the horizontal propagation of quasi-stationary waves. *J. Atmos. Sci.,* **46,** 2802–2811.

Kunkel, K. E., 1989: A surface energy budget view of the 1988 Midwestern United States drought. *Bound. Layer Meteor.,* **48,** 217–225.

Lau, K.-M., and L. Peng, 1992: Dynamics of atmospheric teleconnections during the northern summer. *J. Climate,* **5,** 140–158.

Lettau, H., K. Lettau, and L. C. B. Molion, 1979: Amazonia's hydrologic cycle and the role of atmospheric recycling in assessing deforestation effects. *Mon. Wea. Rev.,* **107,** 227–238.

Livezey, R. E., 1980: Weather and circulation of July 1980—Climax of historic heat wave and drought over the United States. *Mon. Wea. Rev.,* **108,** 1708–1716.

Madden, R. A., and J. Williams, 1978: The correlation between temperature and precipitation in the United States and Europe. *Mon. Wea. Rev.*, **106,** 142–147.

Mintz, Y., 1984: The sensitivity of numerically simulated climates to land-surface boundary conditions. *The Global Climate,* J. T. Houghton, Ed., Cambridge University Press, 79–106.

Mo, K. C., J. Pfaendtner, and E. Kalnay, 1987: A GCM study of the maintenance of the June 1982 block in the Southern Hemisphere. *J. Atmos. Sci.*, **44,** 1123–1142.

——, J. R. Zimmerman, E. Kalnay, and M. Kanamitsu, 1991: A GCM study of the 1988 United States drought. *Mon. Wea. Rev.*, **119,** 1512–1532.

Namias, J., 1960: Factors in the initiation, perpetuation and termination of drought. Extract of Publ. No. 51, IASH Commision of Surface Waters, 81–94.

——, 1962: Influences of abnormal heat sources and sinks on atmospheric behavior. *Proc. Int. Symp. on Numerical Weather Prediction,* Tokyo, Japan, Meteorological Society of Japan, 615–627.

——, 1978: Persistence of United States seasonal temperatures up to one year. *Mon. Wea. Rev.*, **106,** 1557–1567.

——, 1982: Anatomy of Great Plains protracted heat waves (especially the 1980 United States summer drought). *Mon. Wea. Rev.*, **110,** 824–838.

——, 1989: Written in the winds: the great drought of 1988. *Weatherwise,* **41,** 85–87.

——, 1991: Spring and summer 1988 drought over the contiguous United States—causes and prediction. *J. Climate,* **4,** 54–65.

Neilley, P. N., and R. M. Dole, 1991: Interactions between synoptic scale eddies and the large-scale flow during the development of blocking over the North Atlantic ocean. Preprints, *First Int. Symp. on Winter Storms.* New Orleans, LA, Amer. Meteor. Soc., 50–55.

Oglesby, R. J., and D. J. Erickson, 1989: Soil moisture and the persistence of North American drought. *J. Climate,* **2,** 1362–1380.

Palmer, T. N., and C. Brankovic, 1989: The 1988 US drought linked to anomalous sea surface temperature. *Nature,* **338,** 54–57.

Plumb, R. A., 1985: On the three-dimensional propagation of stationary waves. *J. Atmos. Sci.*, **42,** 217–229.

Rasmusson, E. M., 1968: Atmospheric water vapor transport and the water balance of North America. Part II: Large-scale water balance investigations. *Mon. Wea. Rev.*, **96,** 720–734.

Rind, D., 1982: The influence of ground moisture conditions in North America on summer climate as modelled in the GISS GCM. *Mon. Wea. Rev.*, **110,** 1487–1494.

Ropelewski, C. F., 1988: The global climate for June–August 1988: A swing to the positive phase of the southern oscillation, drought in the United States, and abundant rain in monsoon areas. *J. Climate,* **1,** 1153–1174.

Sardeshmukh, P. D., 1988: The generation of global rotational flow by steady idealized tropical divergence. *J. Atmos. Sci.*, **45,** 1228–1251.

——, 1993: The baroclinic χ-problem and its application to the diagnosis of atmospheric heating rates. *J. Atmos. Sci.*, **50,** 1099–1112.

——, and B. J. Hoskins, 1985: Vorticity balances in the tropics during the 1982–83 El Nino-Southern Oscillation event. *Quart. J. Roy. Meteor. Soc.*, **111,** 261–278.

Sellers, W. D., 1965: *Physical Climatology.* The University of Chicago Press, 272 pp.

Schubert, S., M. Suarez, C.-K. Park, and S. Moorthi, 1993: GCM simulations of intraseasonal variability in the Pacific/North American region. *J. Atmos. Sci.*, **50,** 1991–2007.

Shukla, J., and Y. Mintz, 1982: Influence of land-surface evapotranspiration on the earth's climate. *Science,* **215,** 1498–1501.

Shutts, G. J., 1986: A case study of eddy forcing during an Atlantic blocking episode. *Advances in Geophysics,* Vol. 29, Academic Press, 135–164.

Taubensee, R. E., 1980: Weather and circulation of September 1980. *Mon. Wea. Rev.*, **108,** 2100–2106.

Trenberth, K. E., 1986: An assessment of the impact of transient eddies on the zonal flow during a blocking episode using localized Eliassen-Palm flux diagnostics. *J. Atmos. Sci.*, **43,** 2070–2088.

——, and J. G. Olson, 1988: Evaluation of NMC global analyses: 1979–1987. NCAR Tech. Note NCAR/TN-299+STR. NCAR, Boulder, CO, 82 pp.

——, and G. W. Branstator, 1992: Issues in Establishing Causes of the 1988 Drought over North America. *J. Climate,* **5,** 159–172.

——, ——, and P. A. Arkin, 1988: Origins of the 1988 North American drought. *Science,* **242,** 1640–1645.

Wagner, A. J., 1980: Weather and circulation of August 1980—eastward spread of the heat wave and drought. *Mon. Wea. Rev.*, **108,** 1924–1932.

——, 1981: The weather and circulation of 1980. *Weatherwise,* **34,** 5–12.

Wolfson, N., R. Atlas, and Y. C. Sud, 1987: Numerical experiments related to the summer 1980 U.S. heat wave. *Mon. Wea. Rev.*, **115,** 1345–1357.